Mode locking in an infinite set of coupled circle maps

Preben Alstrøm and Risto K. Ritala
Nordisk Institut for Teoretisk Atomfysik (NORDITA), Blegdamsvej 17, DK-2100 Copenhagen Ø, Denmark
(Received 13 June 1986)

We show that the mode locking in coupled circle maps with random phases is very different from that in a single circle map. A finite nonlinearity K_c is needed for a step to appear. The width of the step behaves as $(K-K_c)^2$. The complete mode locking (at $K=1$ for uncoupled maps) behaves singularly as the coupling is turned on. We argue that our model describes the mode locking in charge-density-wave materials. Our results are in qualitative agreement with the experimental observation by Sherwin and Zettl that only few true steps exist in the I-V characteristics and that in addition to these there are some "incomplete" steps.

I. INTRODUCTION

Circle maps are an interesting and important laboratory for studies of nonlinear dynamical phenomena. A circle-map dynamics is an iteration of the form

$$x_{n+1}=x_n+\Omega+Kg(x_n)\ , \tag{1}$$

where the function g is periodic in x:

$$g(x+2\pi)=g(x)\ .$$

The quantity of central interest in studies of circle maps is the rotation number, which tells the average rate of change in the variable x in units of the period of $g(x)$:

$$R=\frac{1}{2\pi}\lim_{n\to\infty}\left[\frac{x_n-x_0}{n}\right]\ . \tag{2}$$

If the rotation number is a rational P/Q, the variable $y_n=x_n \pmod{2\pi}$ has only Q distinct values (asymptotically), whereas if R is irrational the points y_n are dense on $[0,2\pi)$. The motion is said to be mode locked if the rotation number is constant (which can be only a rational) in a region of nonzero area in the parameter (Ω,K) space. The mode locking is complete on a curve $K=K(\Omega)$ if throughout the curve, except on a part of length zero, the motion is mode locked and for infinitely many $R=P/Q$ there is a curve segment of mode locking which has a nonzero length.

Circle maps shows universality in both the complete mode-locking structure[1] and in the onset of chaos through quasiperiodicity.[2,3] Period-doubling bifurcations, onset of bistability, and chaos in regions of mode locking are independent of the specific form of the mapping, too.[1,4] The transition from a mode-locked state to a quasiperiodic motion is through a tangential bifurcation and hence universal.[5] The mode-locking structure, the so-called set of tongues, is characteristic in these systems and mode locking to all rationals is obtained with an infinitesimal nonlinearity (K). Some higher-dimensional continuum dynamical systems are observed to share the universal behavior of circle maps at and below the curve of the complete mode locking. The best-known example is the dynamics of the Josephson junction studied both with digital simulations[6] and with analog devices.[7] (Experiments on subharmonic mode locking in Josephson junctions have so far turned out to be very difficult.[8]) The equivalence holds in many cases even to systems with an infinite number of degrees of freedom. This is because the nontrivial behavior (e.g., changes in the stability) is restricted to a small subspace of the infinite-dimensional state space: In the linearized stability problem the Lyapunov exponents which change sign at the bifurcation span a low-dimensional eigenvector space.[9]

In this paper we study the mode-locking structure of a system with a large number of degrees of freedom, each evolving through a circle map, and coupled linearly to each other. This dynamics is interesting in its own right as a step towards understanding nonlinear dynamical phenomena in many-body systems. The dynamics may be realized in charge-density-wave (CDW) materials under an oscillating external voltage.

The dynamics of impurity-pinned CDW's, which has a natural description in terms of circle maps, does not, at least in all respects, fall into the same category with one-dimensional circle maps. In particular, the depinning of the CDW by electric field is experimentally observed to have a critical behavior different from that of a simple tangential bifurcation.[10] This bifurcation, which is the unlocking transition of the 0/1 step, can be understood only if infinitely many degrees of freedom are taken into account.[11,12]

The Hamiltonian governing CDW motion is[11]

$$H=\frac{J'}{2z}\sum_{i=1}^{N}\sum_{j=1}^{z}(\phi^{(i)}-\phi^{(j)})^2 -\sum_{i=1}^{N}f\cos(\phi^{(i)}+\beta^{(i)})-\sum_{i=1}^{N}E(t)\phi^{(i)}\ . \tag{3a}$$

Here $\phi^{(i)}$ are the phases of the CDW at impurities i, $\beta^{(i)}$ are the pinning phases distributed randomly on a circle, J' the elastic coupling constant, f the pinning strength, and $E(t)$ the external voltage periodic in $\tau=2\pi/\omega$. The second summation of the first term is restricted to the z nearest neighbors of point i. The dynamics is assumed to

be noiseless:

$$m\ddot{\phi}^{(i)}+\dot{\phi}^{(i)}=-\frac{\delta H}{\delta\phi^{(i)}} . \tag{3b}$$

The physical quantity corresponding to the rotation number is the dc part of the current carried by the CDW. $I\sim\langle\dot{\phi}_i\rangle=\omega R$.

We can in principle integrate the Eq. (3b) over τ and obtain a system of coupled circle maps:

$$\phi_{n+1}^{(i)}=\phi_n^{(i)}+\Omega+Kg(\phi_n^{(i)}+\beta^{(i)})-J\left[\phi_n^{(i)}-z^{-1}\sum_{j=1}^{z}\phi_n^{(j)}\right], \tag{4}$$

where the parameters Ω, K, and J and the function g are functions of f and J' and functionals of $E(t)$. Note that we have neglected the velocity return map $\dot{\phi}_{n+1}^{(i)}=F(\phi_n^{(j)},\dot{\phi}_n^{(j)})$, which in the limit of small m is irrelevant.

The connection between the dynamics of Eq. (3) and Eq. (4) is not simple: It is known that if $m=0$ and $J=0$ the continuum version does not have subharmonic mode lockings, whereas Eq. (4) has for almost all functions g finite intervals of Ω with subharmonic lockings. Even though the value of the mass parameter m is estimated to be small[13] the description in terms of circle maps is relevant because the experiments show a rich mode-locking structure.[14] In this paper we study whether in the coupled case, $J\neq0$, the qualitative features of Eq. (4) and the CDW dynamics are the same.[15] We find this to be true indicating that the limit of vanishing J is singular.

From now on we choose $g(x)=-\sin(x)$ in Eq. (4) and, encouraged by the universality results for one degree of freedom, expect this to be generic.

One should appreciate the role of random phases in the dynamics of Eq. (4). Suppose the $\beta^{(i)}$'s were all equal. Then the dynamics has a simple solution with a uniform spatial structure: $\phi_n^{(i)}=\phi_n$. The uniform phases ϕ_n are simply the one-degree-of-freedom values. The stability of the uniform solution is given by the equation

$$\delta\phi_{n+1}^{(i)}=\delta\phi_n^{(i)}-\delta\phi_n^{(i)}K\cos(\phi_n+\beta)-J\left[\delta\phi_n^{(i)}-z^{-1}\sum_{j=1}^{z}\delta\phi_n^{(j)}\right] . \tag{5a}$$

The linear operator on the right-hand side has eigenvalues

$$\lambda=\prod_{n=1}^{Q}[1-K\cos(\phi_n+\beta)-aJ] , \tag{5b}$$

where $\alpha\in[0,2]$ and Q is the periodicity of ϕ_n. These eigenvalues are positive and less or equal to the stability eigenvalue of a single circle map if $2J+K<1$. The mode-locking steps disappear through a tangential bifurcation, which corresponds to a $\lambda=1$. Obviously, the step of the coupled problem exists as long as that of the single degree of freedom in this region of the K,J space. Note that condition for K,J is a sufficient one: In fact, one observes numerically that the edges of the steps are those of the uncoupled problem up to $K\sim1$ for $J\ll0.5$. Period-doubling bifurcations on the step, which correspond to $\lambda=-1$, are different for the coupled system. In addition to uniform solutions there usually coexist nonuniform ones, which have a spatial structure of domains interpolating between the Q different values of the uniform period-Q solution.[16] However, the mode-locking structure of the dynamics, Eq. (4), with the $\beta^{(i)}$'s equal and small J can be understood fairly well in terms of the solution of the one-degree-of-freedom map. In particular one finds mode locking to all rationals with infinitesimal K.

Things are much more complicated for random $\beta^{(i)}$'s: The uniform solution does not exist and the stability problem is not related to the eigenvalue of the linear stability of the one degree of freedom. This has dramatic effects on the properties of the dynamics at the tangential bifurcation point where a P/Q step disappears: The quantity $|R-P/Q|$ behaves as $|\Omega-\Omega_T(P/Q)|^{\zeta}$ with $\zeta>1$,[11,12] whereas $\zeta=\frac{1}{2}$ for one degree of freedom. In this paper we consider this and other effects due to many degrees of freedom and spatial inhomogeneity.

This paper is organized as follows: In Sec. II we introduce the technique of the infinite range of elastic interactions ($z\rightarrow\infty$), which is a simple generalization of the one derived by Fisher.[11] This approximation allows us to have a nice analytic handle on the mode-locking structure. Section III discusses our results for the phase diagram of the Fibonacci steps in K,J plane. We prove that a finite $K=K_c$ is needed for a step to appear for any nonzero J. The decay of the step sizes is found to be universal close to K_c. The positions of the first period-doubling lines on the step are determined. There exist parameter ranges where period-doubling precedes the appearance of the step. All these results have been obtained both for the infinite-range model and in simulations on a two dimensional (2D) square lattice with nearest-neighbor interactions. Section IV studies J as a small perturbation on the Fibonacci steps at $K=1$, the complete mode-locking line of the uncoupled map. We find that J is more relevant variable than $1-K$. We have not been able to determine the complete mode-locking line for any nonzero J; we cannot even show that it exists. Calculations are carried out again both in the infinite-range approximation and on the 2D square lattice. In Sec. V we study the disappearance mechanism of the steps, which is a new kind of tangential bifurcation. The leading correction[12] to the infinite-range approximation is shortly discussed. The paper is concluded in Sec. VI by discussing the relevance of the return-map dynamics, and in particular the infinite-range model, to the CDW dynamics.

II. INFINITE-RANGE APPROXIMATION

The dynamics of Eq. (4) is in general too difficult to be discussed analytically. Therefore, as an alternative to our numerical simulations, we adopt the infinite-range approximation, first used in CDW context by Fisher.[11] In this approximation all the spatial degrees of freedom $\phi_n^{(i)}$ are coupled to each others with a coupling constant inversely proportional to the number of degrees of freedom N. For ordinary phase transitions, such as in ferromagne-

tism, this approximation is exactly the mean-field theory because both approaches neglect the spatial fluctuations of the order parameter. Then one usually finds that there exists an upper spatial critical dimension d_c such that systems with $d > d_c$ show universal critical properties equal to those of the infinite-range approximation. Recently, it has been argued that the onset of sliding motion in CDW's, which corresponds to the disappearance of the 0/1 step in Eq. (4), has an infinite critical dimensionality d_c.[12] Therefore, here the status of the infinite-range approximation is unclear, but this approximation has to be worked out before the fluctuation effects can be considered.

The infinite-range approximation in Eq. (4) means that we replace the number of nearest neighbors z by the number of degrees of freedom N. Then in the thermodynamical limit, $N \to \infty$, we find that

$$\frac{1}{N}\sum_{j=1}^{N}\phi_n^{(j)} = \langle \phi_n \rangle \ , \tag{6}$$

where the angular brackets denote average over space, or equivalently, over the configurations of $\beta^{(i)}$'s.

The most general ansatz for $\langle \phi_n \rangle$, when the rotation number is a rational $R = P/Q$ and the orbit has periodicity Q, is

$$\langle \phi_n \rangle = n 2\pi P/Q + C_{n \ (\mathrm{mod}\, Q)} \ , \tag{7}$$

where the numbers $\{C_n\}_{i=1}^{i=Q}$ are constants.

Combining Eqs. (6) and (7) with Eq. (4) we find a local equation of motion for each $\phi_n^{(i)}$:

$$\phi_{n+1}^{(i)} = \phi_n^{(i)} + \Omega - K\sin(\phi_n^{(i)} + \beta^{(i)}) - J(\phi_n^{(i)} - n 2\pi P/Q - C_{n \ (\mathrm{mod}\, Q)}) \ . \tag{8}$$

The solution of Eq. (8) has to satisfy the condition (7). The effects due to an infinite number of degrees of freedom are translated into that Eqs. (7) and (8) must be consistent.

It is useful to write $\phi_n^{(i)} = n 2\pi P/Q + C_{n \ (\mathrm{mod}\, Q)} + x_n^{(i)}$. Then Eq. (8) for the derivations from the (spatial) average value of the phases, $x_n^{(i)}$, reads as

$$x_{n+1}^{(i)} = (1-J)x_n^{(i)} + \Omega - 2\pi P/Q + C_{n \ (\mathrm{mod}\, Q)} - C_{n+1 \ (\mathrm{mod}\, Q)} - K\sin(x_n^{(i)} + n 2\pi P/Q + C_{n \ (\mathrm{mod}\, Q)} + \beta^{(i)}) \ . \tag{9}$$

Obviously, $x_n^{(i)}$ is bounded as $n \to \infty$ if J is in the interval (0,2), and hence the part linear in n in the self-consistency condition, Eq. (7), is always satisfied. The consistency requirement for the Q points of the stable period-Q orbit of Eq. (9) for a given $\beta^{(i)}$, $\{x_n^{*(i)}(\beta^{(i)})\}_{n=1}^{n=Q}$, reduces to

$$\frac{1}{2\pi}\int_0^{2\pi} d\beta^{(i)} x_n^{*(i)}(\beta^{(i)}) = 0 \text{ for } n = 1,2,\ldots,Q \ . \tag{10}$$

(Because the equations are local we shall from now on neglect the spatial indices.)

In this paper we confine ourselves to solutions for which all the constants C_n are equal. This is self-consistent in that if we first choose all the constants $C_n = C$, C some number, solve the set of Eqs. (9), and find the new constants C_n' through

$$C_n' = C + \frac{1}{2\pi}\int_0^{2\pi} d\beta x_n^*(\beta) \ \text{ for } n = 1,2,\ldots,Q \tag{10'}$$

these will all be equal. Hence the choice of just one constant C is justified. If we denote the above connection between C' and C by $C' = f(C)$, the self-consistency is obtained through the fixed points of this relation: $C^* = f(C^*)$.

The equality of the constants C_n' in Eq. (10') is a consequence of the symmetries of the problem: Shifting the random phases uniformly, $\beta^{(i)} \to \beta^{(i)} + m 2\pi P/Q$, m a positive integer and smaller than Q, shifts the time labels of the curves $\{x_n^*(\beta)\}_{n=1}^{n=Q}$ by $n \to n+m \ (\mathrm{mod}\, Q)$ $(Q-m \to Q)$. The random phases $\beta^{(i)}$ are defined only mod 2π, and therefore the β shifts do not affect integrals over $[0,2\pi)$:

$$\int_0^{2\pi} d\beta x_1^*(\beta) = \int_0^{2\pi} d\beta x_2^*(\beta - 2\pi P/Q) = \cdots = \int_0^{2\pi} d\beta x_Q^*(\beta - (Q-1)2\pi P/Q) \ . \tag{11}$$

In the special case of $P/Q = \frac{1}{2}$ it is easy to show that the solution with $C_1 = C_2$ is the only self-consistent solution, and we expect that these are the dominating ones on any P/Q step before the period-doubling bifurcations occur.

We have freedom in choosing the self-consistent value of the constant C^*. Two different values are related by a uniform shift in random phases. From now on we choose $C^* = 0$. Then the dynamics, Eq. (8), is simplified into

$$x_{n+1}^{(i)} = (1-J)x_n^{(i)} + Q - 2\pi P/Q - K\sin(x_n^{(i)} + n 2\pi P/Q + \beta^{(i)}) \ . \tag{12}$$

Because of the symmetries under uniform β shifts by $m 2\pi P/Q$, it is equivalent to study one of the curves $x_n^*(\beta)$ at $\beta \in [0,2\pi)$ or all of them at $\beta \in [0,2\pi/Q)$:

$$\frac{1}{2\pi}\int_0^{2\pi} d\beta x_1^*(\beta) = \frac{1}{2\pi}\int_0^{2\pi/Q} d\beta \sum_{n=1}^{Q} x_n^*(\beta) \ . \tag{13}$$

The second form is especially useful when the curves $x_n^*(\beta)$ have to be determined numerically.

We note yet another symmetry of the dynamics in Eq. (12). The following transformation,

$$Q \to \Omega + \Delta\Omega \ , \tag{14a}$$

$$x_n^{(i)} \to x_n^{(i)} + \frac{\Delta\Omega}{J} \ , \tag{14b}$$

$$\beta^{(i)} \to \beta^{(i)} - \frac{\Delta\Omega}{J} \ , \tag{14c}$$

leaves the equation unchanged. Using again the fact that uniform shifts in random phases do not affect integrals over $[0,2\pi)$ we find that

$$\frac{1}{2\pi}\int_0^{2\pi/Q} d\beta \sum_{n=1}^{Q} x_n^*(\beta, \Omega + \Delta\Omega) = \frac{1}{2\pi}\int_0^{2\pi/Q} d\beta \sum_{n=1}^{Q} x_n^*(\beta,\Omega) + \frac{\Delta\Omega}{J} \ . \tag{15}$$

This relation is useful in determining the value of Ω corresponding to the rotation number P/Q: We need to evaluate the curves $\{x_n^*(\beta)\}_{n=1}^{n=Q}$ only for one Ω.

III. MODE-LOCKING STEPS IN PARAMETER SPACE

The mode-locking structure of the dynamics, Eq. (4), is well-known for the uncoupled case $J=0$. In the (Ω,K) plane there exist "tongues" for each rational rotation number P/Q, such as the one displayed in Fig. 1, having the following properties.[1-4]

(i) The tongues exist down to $K=0$. The width of the tongues vanishes continuously as K^Q, when $K\to 0$.[17]

(ii) The width of a tongue is nonzero for all positive K.

(iii) $K=1$ is the complete mode-locking line.

(iv) Above the complete mode-locking line there exist hyperbola-shaped curves $K=K_{\rm pd}^{(n)}(\Omega)$, $n=1,2,\ldots,\infty$, such that in the regime between curves $K_{\rm pd}^{(n)}(\Omega)$ and $K_{\rm pd}^{(n+1)}(\Omega)$ the periodicity is 2^nQ and the rotation number $R=P/Q$ (usually denoted as $2^nP/2^nQ$). On yet another curve $K=K_d(\Omega)$ there coexist infinitely many rotation numbers, which lead to irregular motion.

In this section we study how properties (i), (ii), and (iv) are changed when J is turned on. We discuss both the infinite-range approximation and our simulations on a two-dimensional square lattice.

A. Infinite-range approximation

The condition for mode locking in the infinite-range model is that the self-consistency condition, Eq. (10), is satisfied in an Ω interval of nonzero measure. Let us first assume that the curves $\{x_n^*(\beta)\}_{n=1}^{n=Q}$ are single-valued, as in Fig. 2. If the motion is locked in the vicinity of $\Omega=\Omega_0$, there exists, by definition, a nonzero $\Delta\Omega$ such that the condition of Eq. (10) is satisfied for both Ω_0 and $\Omega_0+\Delta\Omega$. But when we insert these values of parameters into Eq. (15) and note that because of the Eq. (10) the integrals on both sides have to vanish, we find that a vanishing $\Delta\Omega$ is the only self-consistent solution. Therefore there exist no mode-locking steps for single-valued $\{x_n^*(\beta)\}_{n=1}^{n=Q}$.

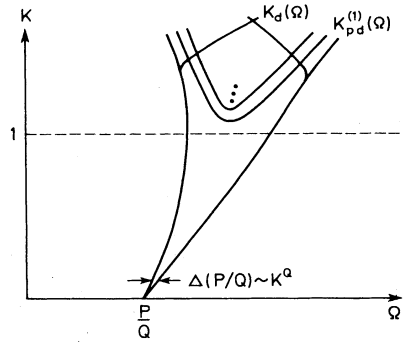

FIG. 1. Structure of mode-locking tongue P/Q of uncoupled circle maps as explained in text.

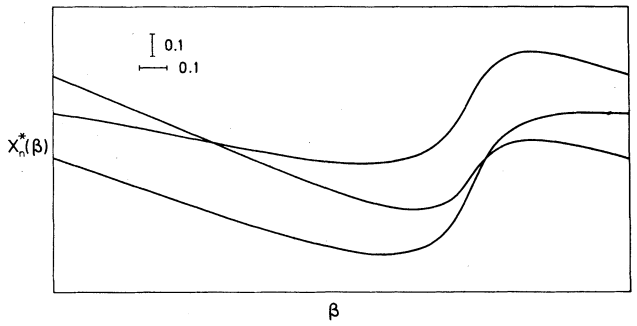

FIG. 2. Curves $x_n^*(\beta)$ for $P/Q=\frac{1}{3}$ below $K_c=0.448$; $J=0.03$, $K=0.4$.

If the curves are multivalued, as those shown in Fig. 3, it is possible to combine the branches for different Ω's in different ways to ensure self-consistency in an interval in Ω of finite measure. Furthermore, even for a fixed Ω in this interval there is a continuum of combinations of the branches such that each combination obeys condition (10). Thus at each point on the step an infinity of metastable mode-locked solutions with equal rotation numbers coexist. This should manifest itself as hysteresis and long relaxation times in experiments and simulations.

The transition from single-valuedness to multivaluedness at some $K=K_c(J)$ is through a bifurcation (without period-doubling) of the family of orbits $\{x_n^*(\beta)\}_{n=1}^{n=Q}$, also called the cusp catastrophe.[18] This means that at some value of β the linear stability eigenvalue λ is

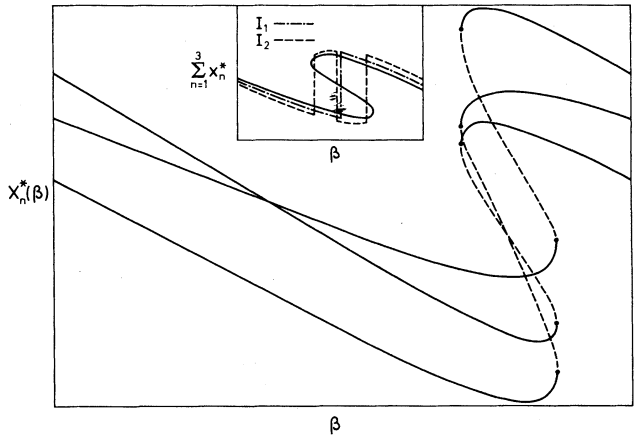

FIG. 3. Curves $x_n^*(\beta)$ for $P/Q=\frac{1}{3}$ above $K_c=0.448$; $J=0.03$, $K=0.55$. Scale is as in Fig. 2. Dashed part is unstable branch. We have inset a figure which illustrates combinations of stable branches in integrals I_1,I_2 such that they yield the same Ω's through the self-consistency condition even though the combinations correspond to different solutions.

$$\lambda=\prod_{n=1}^{Q}\{1-J-K_c(J)\cos[x_n^*(\beta)+n2\pi P/Q+\beta]\}=1\ , \tag{16}$$

and otherwise $\lambda<1$ indicating a supercritical double point at this value of β. As the nonlinearity parameter K is further increased from $K_c(J)$ one finds an interval in β with one unstable branch $\{x_n^{*0}(\beta)\}_{n=1}^{n=Q}$ and two stable branches $\{x_n^{*<,>}(\beta)\}_{n=1}^{n=Q}$, as is shown in Fig. 3. The new branches arise through a turning point.[9] The cusp catastrophe is displayed in Fig. 4.

We have determined the curves $K_c(J;Q)$ for lowest-order Fibonacci steps ($m=0,1,\ldots,5$), $R=F_m/F_{m+2}$, where $F_0=0$, $F_1=1$, and $F_{m+1}=F_m+F_{m-1}$ for $m\geq 1$. We have chosen Fibonacci steps because we are interested in what happens as $Q\to\infty$ and earlier works[2-4] have shown that the asymptotic behavior is found most rapidly for the Fibonacci sequence. (The scaling behavior of various properties depends on the sequence of rationals studied. By studying only Fibonacci steps we limit ourselves to scaling in a neighborhood of irrationals with continued-fraction representation[3] having the same tail as the golden mean, i.e., equivalent to it.)

The critical curves are extremely well described by the expression

$$K_c(J;Q)=(QJ)^{1/Q} \tag{17}$$

up to $K_c=O(1)$, over 3 orders of magnitude in J in our numerical results for $\{x_n^*(\beta)\}_{n=1}^{n=Q}$. The difference between Eq. (17) and the numerical results is shown in Fig. 5. The errors seem to be insensitive to m for $m>2$. The result, Eq. (17), is exact for $m=0$ and can be shown to coincide with the leading term of small-J expansion of $m=1$.

The width of the step in Ω for values of K slightly larger than the critical value can be determined from the cusp catastrophe picture, too. The starting (end) point $\Omega_<$ ($\Omega_>$) of the mode-locking interval is determined by choosing the upper (lower) branch of the curve $\sum_{n=1}^{Q}x_n^{*>(<)}(\beta)$ throughout the multivalued region. The width $\Delta\Omega=\Omega_>-\Omega_<$ is obtained through the definitions of $\Omega_<$ and $\Omega_>$ and Eq. (15):

$$\begin{aligned}0&=\frac{1}{2\pi}\int_0^{2\pi/Q}d\beta\sum_{n=1}^{Q}x_n^{*>}(\beta;\Omega_<)\\&=\frac{1}{2\pi}\int_0^{2\pi/Q}d\beta\sum_{n=1}^{Q}x_n^{*>}(\beta;\Omega_>)-\frac{\Delta\Omega}{J}\\&=\frac{1}{2\pi}\int_{\beta_1}^{\beta_2}d\beta\sum_{n=1}^{Q}[x_n^{*>}(\beta;\Omega_>)-x_n^{*<}(\beta;\Omega_>)]-\frac{\Delta\Omega}{J}\ ,\end{aligned} \tag{18}$$

where β_1,β_2 are the end points of the multivaluedness interval in β. According to Eq. (18) the width of the mode-locking interval is proportional to the area of the "hysteresis" loop of $\sum_{n=1}^{Q}x_n^*(\beta)$ multiplied by the coupling constant J.

Close to the critical curve $K_c(J)$ the inverse of the function $x=F(\beta)=\sum_{n=1}^{Q}x_n^*(\beta)$ can, following the standard catastrophe theory, be written as

$$\begin{aligned}\beta-\beta_0&=F^{-1}(x)-\beta_0\\&=a(J,K;Q)(x-x_0)+b(J,K;Q)(x-x_0)^3\ .\end{aligned} \tag{19}$$

Here (β_0,x_0) is the point where the stability is lost at $K=K_c(J)$. A second-order term is forbidden, because it would not describe a cusp catastrophe but a transcritical double point. At the critical curve the coefficient $a(J,K;Q)$ vanishes. The width of the multivalued region $\beta_2-\beta_1$ is proportional to $a^{3/2}$ and the difference between the two stable branches, $x_n^{*>}-x_n^{*<}$, to $a^{1/2}$. Hence the area of the loop behaves as a^2.

There is no *a priori* reason to expect that the point $(K_c(J),J)$ is a special point of a $(J,K;Q)$. We keep J fixed and expand in K: $a(J,K;Q)=a_1(J;Q)(K-K_c)+O((K-K_c)^2)$, which yields the leading contribution

$$\Delta\Omega\sim(K-K_c)^2\ . \tag{20}$$

This is to be contrasted with the Q-dependent scaling,

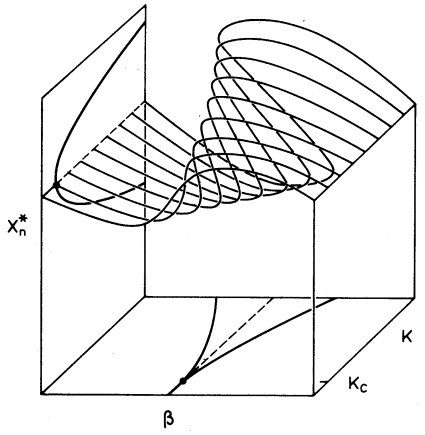

FIG. 4. Cusp catastrophe. Projections show how difference of the branches and width of multivalued region in β depend on K.

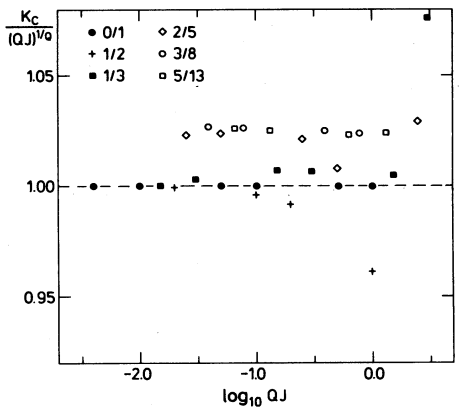

FIG. 5. Ratio of numerically determined values of $K_c(J)$ to one obtained from Eq. (17).

property (i) of uncoupled circle maps. The quadratic dependence, Eq. (20), is in excellent agreement with numerically determined $\{x_n^*(\beta)\}_{n=1}^{n=Q}$.

At the point $(K,J)=(0,0)$ there is crossover. This can be explained by assuming that the coefficient a_1 diverges as $(QJ)^{-1/Q}=K^{-1}$ as $J\to 0$. Then according to the discussion above

$$\Delta\Omega\sim Ja^2\sim Q^{-1}K^Q\left[\frac{K-K_c}{K}\right]^2\to K^Q \text{ as } K_c\to 0 \qquad (20')$$

which recovers the uncoupled behavior.

Since the result, Eq. (20), follows directly from the cusp catastrophe, it holds for all choices of smooth $g(x)$ in Eq. (4) and is hence universal. However, our result on the critical nonlinearity, Eq. (17), has been derived only for $g(x)=-\sin x$, so we do not know whether this is universal or not.

Another breakdown of the single-valuedness of the curves $\{x_n^*(\beta)\}_{n=1}^{n=Q}$ is through a period-doubling bifurcation, which occurs either on single-valued curves (and hence prior to the mode locking, which is not possible at $J=0$) or after the cusp point. Period-doubling means here that at some value of β the linear stability eigenvalue λ is

$$\lambda=\prod_{n=1}^{Q}\{1-J-K_{\rm pd}^{(1)}(J)\cos[x_n^*(\beta)+n2\pi P/Q+\beta]\}=-1 \qquad (21)$$

and $\lambda>-1$ otherwise. At values of K larger than $K_{\rm pd}^{(1)}(J)$, defined through Eq. (21), the dynamics, Eq. (12), has a solution with periodicity $2Q$ instead of Q in an interval in β. Thus there are $2Q$ curves $\{x_n^*(\beta)\}_{n=1}^{n=2Q}$ which must satisfy the self-consistency condition, Eq. (10). There exist no symmetries relating the curves $x_n^*(\beta)$ and $x_{n+Q}^*(\beta)$ in the interval $\beta\in[0,2\pi)$ (only in the "unphysical" interval $[0,4\pi)$). Therefore we expect that in general

$$\frac{1}{2\pi}\int_0^{2\pi}d\beta\, x_n^*(\beta)\neq\frac{1}{2\pi}\int_0^{2\pi}d\beta\, x_{n+Q}^*(\beta) \qquad (22)$$

which we have observed also numerically. Equation (22) means that the solution is not self-consistent. We have to allow an oscillating part in the ansatz for the average phase and hence break the translational symmetry in time by employing $2Q$ coefficients to satisfy the self-consistency:

$$\langle\phi_n^{(i)}\rangle=n2\pi P/Q+C_{n\,(\mathrm{mod}\,2Q)}\,,\quad C_n\neq C_{n+Q}\,. \qquad (7')$$

The $2Q$ self-consistency conditions for variables $x_n^{(i)}=\phi_n^{(i)}-\langle\phi_n\rangle$ are then Eq. (10). The widths of the steps and the period-doublings into $4Q$-periodic orbits can be studied in the same way as we discussed above for the Q-periodic solution. We do not carry out the analysis of $2Q$-periodic motions in this paper.

If the point β_0, where the period-doubling occurs first, is on the single-valued part of the curve $\sum_{n=1}^{Q}x_n^*(\beta)$, which is multivalued in some other part (and hence corresponds to a step), the period-doubling cannot be avoided by any special choice of the branches, or, equivalently, at any Ω on the step. Thus the critical line, $K=K_{\rm pd}^{(1)}(\Omega;J)$, of the period-doubling is independent of Ω. This is in contrast to the hyperbola observed in the uncoupled system [see property (iv)]. When we determined the curves $\{x_n^*(\beta)\}_{n=1}^{n=Q}$ numerically for the lowest-order ($m<6$) Fibonacci steps, we found that period-doubling bifurcation intervals always opened up at the single-valued regions of the curves.

For small enough J there exist two or more stable branches throughout the interval $[0,2\pi)$ and thus some choices of the branches avoid the period-doubled part, which does not appear simultaneously on all the branches. Even then there coexist period-doubled solutions at all Ω's. The fraction of these vanishes as the edge of the step is approached and hence in experiments and in numerical simulations one should observe an effective $K_{\rm pd}^{(1)}$ which is curved and dependent on the observation procedure.

The mechanism of the period-doubling bifurcation as a function of β and the parameters is displayed in Fig. 6. The stability eigenvalue, Eq. (21), as a function of β close to the bifurcation curve $K_{\rm pd}^{(1)}$ and to the point β_0 where the stability is lost first can be written as

$$\lambda(\beta)=-1+A+B(\beta-\beta_0)^2\,, \qquad (23)$$

where $A=0$ is the period-doubling line. Expanding A in $K-K_{\rm pd}^{(1)}(J)$ and taking into account only the linear term we find that width of the period-doubled region is proportional to $[K-K_{\rm pd}^{(1)}(J)]^{1/2}$. Since Eq. (23) is a generic form, i.e., independent of the choice of the function $g(x)$, this result is universal. This behavior is confirmed by our numerical studies of the curves $\{x_n^*(\beta)\}_{n=1}^{n=Q}$. Equation (23) is helpful in locating the period-doubling line numerically.

The period-doubling lines on the lowest-order Fibonacci steps are displayed in Fig. 7. We cannot approximate this set of curves with any simple function which would cover all the values of Q. The positions of the minima of these curves, $J_1(Q)$, seem to behave as Q^{-1} with a prefactor larger than one. This means that the minima are always

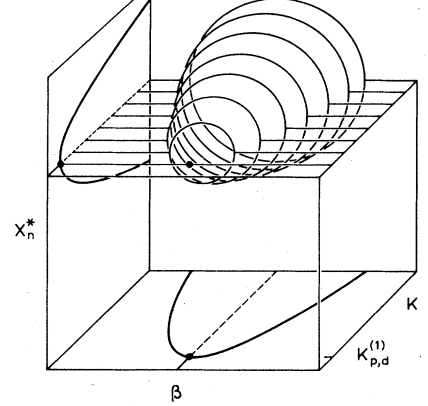

FIG. 6. Period-doubling bifurcation of curves $x_n^*(\beta)$. Projections show how difference of the branches and width of period-doubled in β depend on K. Period-doubled orbit alternates between branches at fixed β and K. We have drawn the part which is not bifurcated as a horizontal line for simplicity.

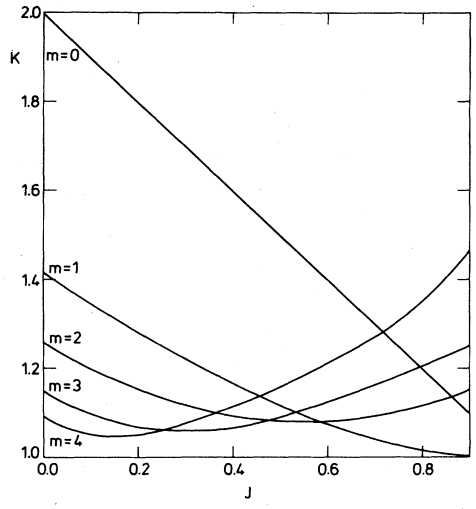

FIG. 7. Curves $K_{pd}^{(1)}(J)$ for lowest-order Fibonacci steps F_m/F_{m+2}, $m=0,\ldots,4$.

above J_0, defined as $K_c(J_0)=1$, and thus the period-doubling line and the critical curve have an intersection point in the interval (J_0,J_1). (The period-doubling line always lies above $K=1$ and the value of K at the minimum tends towards 1 as $Q\to\infty$.) For large J the period-doubling line diverges faster than $J^{1/Q}$ indicating another intersection point in (J_1,∞). (However, remember that stability against diverging solutions limits us to $J<2$.)

The generic behavior of the critical curve and the period-doubling line is shown in Fig. 8. Let us now compare the mode-locking tongue of a single circle map (Fig. 1) to the structure indicated by Fig. 8. Two possibilities exist: If $J\in(0,J_<)$ or $J\in(J_>,\infty)$ [Fig. 9(a)] we find at small values of K that the rotation number $R=P/Q$ exists only at one Ω; then at $K=K_c(J)$ the step appears and finally at $K=K_{pd}^{(1)}(J)$ the orbit bifurcates, doubling the

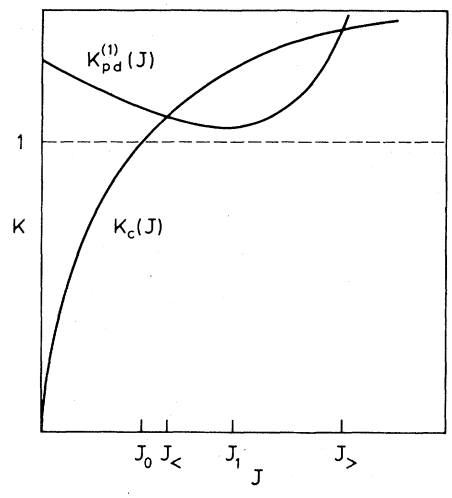

FIG. 8. Generic curves $K_c(J)$ and $K_{pd}^{(1)}(J)$ for a given step P/Q. Indicated values of J are explained in text.

periodicity. At this point we cannot exclude a cusp in the width of the step because of the sudden increase of the self-consistency conditions. If $J\in(J_<,J_>)$ [Fig. 9(b)] the rotation number exists only at one point in Ω until it bifurcates into a $2Q$-periodic orbit. For even larger K, not obtainable from our calculations, the step opens up. More than one period-doubling bifurcation may occur before the step appears [Fig. 9(c)]. In all cases of Fig. 9 the steps lie inside the region of the uncoupled step, Fig. 1. We believe that these qualitative features are universal.

Figures 8 and 9 summarize our analysis of the mode-locking tongue in the infinite-range approximation. All this has been obtained analytically, except that the stable orbits as a function β have to be determined numerically.

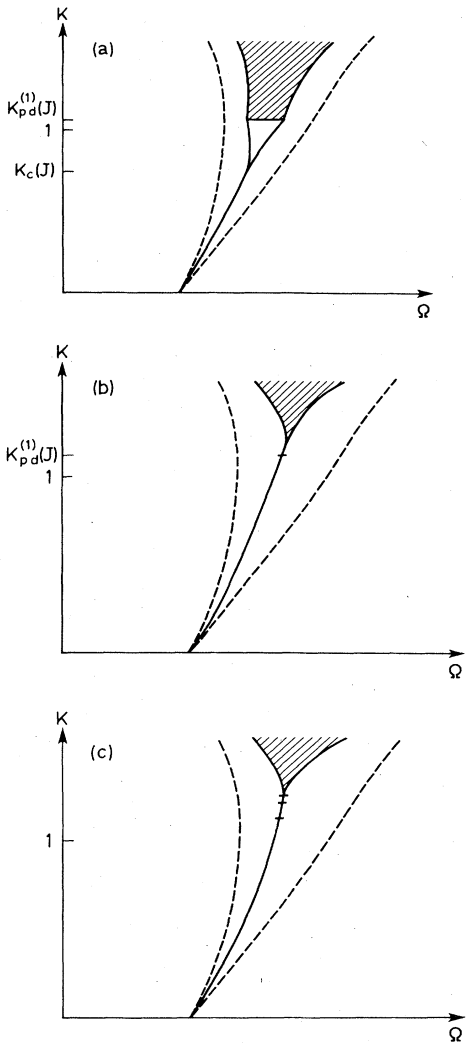

FIG. 9. Structure of mode-locking step at $J\neq 0$. Hatched region indicates that orbit has periodicity 2^nQ, $n>0$, or chaotic. Small horizontal lines below the opening of the step denote period-doubling. (a) Step appears before first period-doubling (at period-doubling the boundary of step may have cusp); (b) one period-doubling before step opens up; (c) several period-doublings before step opens up. Dashed lines are the boundaries of the step for $J=0$, see Fig. 1.

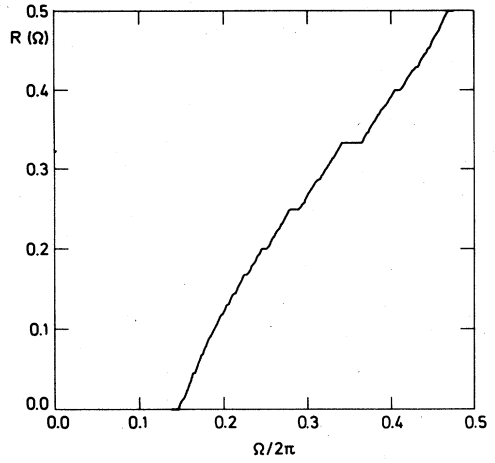

FIG. 10. Rotation number $R(\Omega)$ for $K=1$ and $J=0.04$.

B. Simulations on 2D square lattice

In order to study the effects of finite dimensionality we have carried out numerical simulations of Eq. (4) on a two-dimensional square lattice of size 30×30 with nearest-neighbor couplings ($z=4$) and periodic boundary conditions. The mode-locking structure is investigated by calculating the rotation number R through Eq. (2) with x_n defined as

$$x_n=\frac{1}{N}\sum_{i=1}^{N}\phi_n^{(i)}\,, \tag{24}$$

where N is the number of degrees of freedom, $N=900$.

Figure 10 shows an example of the mode-locking structure obtained through simulations. The value of K is set equal to one, which corresponds to the complete mode-locking line of the uncoupled case, and $J=0.04$. The rotation number is calculated at $\Omega=\Omega_m=0.87+0.01m$ with $m=0,1,2,\ldots,209$ and with a number of iterations $N_{\rm it}=3000$. The 0/1 step is left at $\Omega=0.93$, and $R=1/2$ is reached at $\Omega=2.94$; between these values many steps show up. For rationals with a continued-fraction sum S less than or equal to 5 (see Fig. 11), and for 1/6, we observe flat steps, whereas a finite but small slope can be seen for rationals with $S=6$. For larger values of S we do not find any steplike structure.

The disappearance of steps is studied by keeping J fixed and decreasing the value of the parameter K. Figure 12

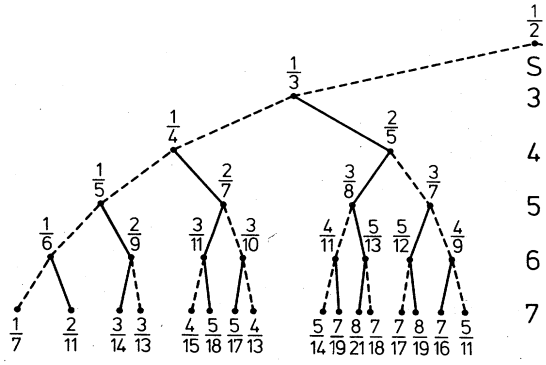

FIG. 11. Farey tree below 1/2 for continued-fraction sum $S<8$. Dashed-line sections are used when the number N of continued-fraction elements is unchanged, while solid-line sections are used when N increases by one.

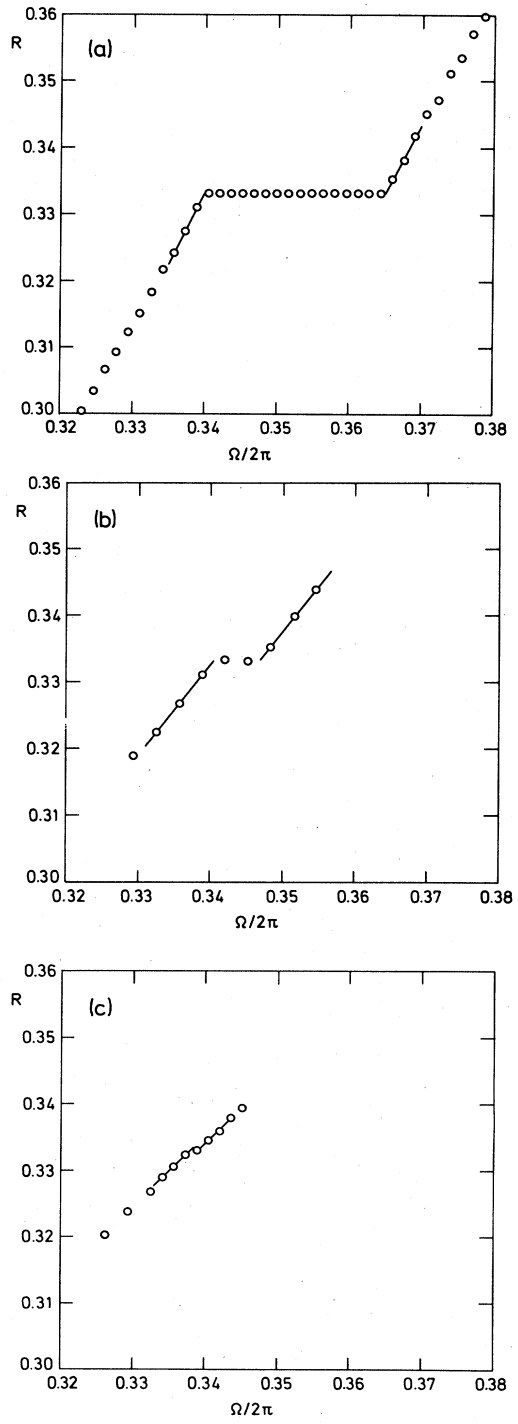

FIG. 12. Rotation number R close to $R=1/3$ for $J=0.04$ and (a) $K=1.0$, (b) $K=0.7$, and (c) $K=0.5$. The lines are least-squares fits. The crossing points with $R=1/3$ determine the step size.

shows the features at the rational $1/3$ for $K=1.0$, 0.7, and 0.5. The lines are the least-squares fits to the points below and above the step and their crossing point with $R=1/3$ determines the stepsize. We notice that the slopes above and below the step are found equal within the numerical accuracy. From these calculations we find that

$$\Delta\Omega \sim (K-K_c)^{\alpha} \tag{25}$$

with $K_c=0.31$ and $\alpha=2.4$, which is to be compared with Eq. (20). Figure 13 displays a log-log plot of the step size versus $K-K_c$ including points between $K=0.50$ and 0.70. A least-squares fit to the behavior of Eq. (25) still yields $\alpha=2.4$. However, there are three sources of systematic error which may explain the discrepancy between this result and Eq. (20): We cannot be sure that the values of K we have chosen are close enough to the critical value for scaling to hold. We simulate a system of fixed finite size; proper finite-size scaling may be necessary. We also assumed that $R(\Omega)$ is linear close to the edges of the steps; a more general power law may be needed when α is to be determined (cf. Sec. V).

We note that K_c is clearly smaller than the value for the infinite-range case, predicted by Eq. (17). This is observed for other steps as well, e.g., $K_c \sim 0.14 < (2J)^{1/2}$ for $R=1/2$. We expect this in analogy to the suppression of the transition temperature by smooth short-range fluctuations in ordinary phase transitions. However, the steps always lie inside the tongues found at $J=0$.[1]

We simulated also the period-doubling structure above the line $K=1$. Figure 14(a) shows that for $R=1/3$ and $J=0.04$ the period-doubling occurs first at the center of the step and then moves towards the edges as is known for $J=0$.[19,20] However, the broadening of the period-doubling interval is much faster at $J\neq 0$. Note that even though infinite-range approximation predicts that $2Q$-periodic solutions exist throughout the step, the curved shape of the period-doubling line in Fig. 14(a) can be understood in terms of coexisting Q-periodic solutions. These are more common near the edges than at the center.

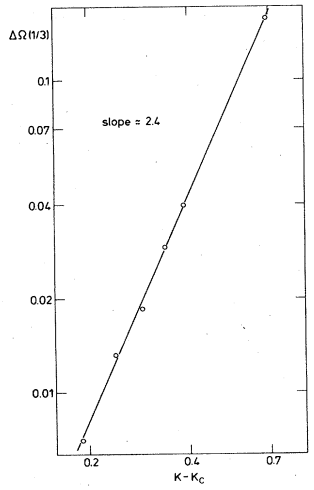

FIG. 13. Double-logarithmic plot of step size of the 1/3 step versus $K-K_c$. $K_c=0.31$ and $J=0.04$. A least-squares fit to Eq. (25) gives $\alpha=2.4$.

The value $K=1.23$ where the period-doubling on the $1/3$ step is seen first is in good agreement with the value $K_{pd}^{(1)}$ found at $z=\infty$ for $J=0.04$.

In accordance with the infinite-range case we observe horizontal period-doubling line for large J. In Fig. 14(b) the step size for $R=1/3$ is shown for $J=0.4$, and here a horizontal line at $K=1.10$ indicates that period-doubling occurs all over the step for $K>1.10$ whereas it is absent for $K<1.10$. The value $K=1.10$ is recovered in the infinite-range case.

IV. $K>1$ AND COMPLETE MODE LOCKING

In this section we study complete mode locking, property (iii) mentioned in the beginning of Sec. III. We are especially interested in what happens close to irrationals equivalent to the golden mean.

Let us for a moment neglect period-doubling and their effects on the widths of the steps, and take the approximate expression for $K_c(J)$, Eq. (17), literally. Figure 15 shows K_c as a function of Q. This curve strikingly has a maximum at $Q'(J)=e/J$, which means that if K is slightly above 1 there is a gap in the mode-locking structure: Steps with $Q\in[Q_1,Q_2]$ are absent but the rest of them are there. The mode-locking structure is perturbed singularly near $K=1$ when J is turned on. Thus the complete mode-locking curve, if one exists, is very different from that of a single circle map and may therefore have a different fractal dimension.

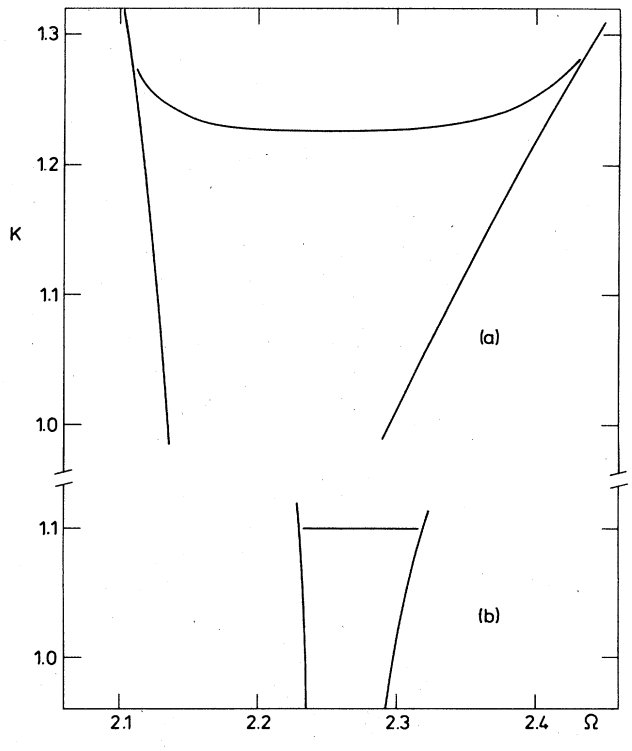

FIG. 14. Mode-locking curve and curve for period-doubling region for the 1/3 step. (a) $J=0.04$. (b) $J=0.4$.

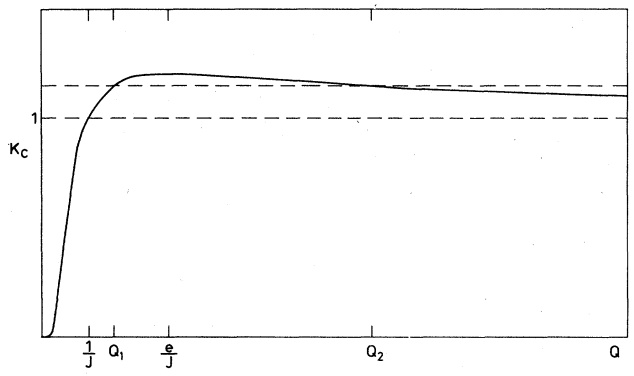

FIG. 15. Critical nonlinearity as a function of Q for Fibonacci steps as given by Eq. (17).

We have studied the effect of small J on the steps at $K=1$ also without using Eq. (17) directly. We fitted our results for the width of the lowest-order ($m<8$) Fibonacci steps obtained from $\{x_n^*(\beta)\}_{n=1}^{n=Q}$ and numerical simulations on a two-dimensional square lattice by the formula

$$\Delta\Omega(Q,J)=\Delta\Omega(Q,0)\exp[-g(Q)J]\ . \tag{26}$$

[It is advantageous to use an exponential rather than linear correction; we find this to be valid up to $g(Q)J=O(1)$.] This is to be compared with the effect of changing K from the complete mode-locking line $K=1$ at $J=0$ ($\varepsilon=1-K$) (Ref. 20):

$$\Delta\Omega(Q,\varepsilon,J=0)=\Delta\Omega(Q,0,0)\exp[-f(Q)\varepsilon] \tag{27}$$

where $f(Q)\sim Q^{\nu}$, with $\nu=1.054$.[2]

One must be cautious when applying Eq. (26) in the limit of infinite Q because a simple exponential on J can be valid only if $J\ll 1/Q$. However, we proceed by using the form Eq. (26), but bear in mind the possible complications as $Q\to\infty$.

It is of great importance whether J is more or less relevant variable than ε. Suppose $g(Q)\sim Q^{\nu'}$. If $\nu'<\nu$ it is possible to restore the width of the step at finite J by a negative $\varepsilon=-AQ^{\nu'-\nu}J$, where A depends on the prefactors of $f(Q)$ and $g(Q)$. Because this correction would then vanish in the limit of infinite Q, it would mean that the complete mode-locking curve would touch $K=1$ at irrationals equivalent to the golden mean [or as Eq. (26) holds only in the limit of vanishing J as Q tends to infinity, the complete mode-locking curve moves smoothly out from $K=1$ as J is turned on]. However, we find the opposite case. Figure 16 displays our results for $g(Q)$, both in the infinite-range approximation and for simulations on a two-dimensional square lattice. In the infinite-range approximation, where the errors are smaller, we find $\nu'=1.16\pm0.02$, clearly larger than ν. The result of the simulations is somewhat more unclear. The exponent ν is known to be universal. Whether ν' is or is not we do not know.

We have not been able to settle the question of the existence of a complete mode-locking curve in the infinite-range approximation because it is difficult to satisfy the self-consistency conditions for period-doubled solutions, which may affect the curve, and because we know of no special features characterizing the complete mode locking. It is too tedious to determine the curve straightforwardly by finding the crossings of all the steps. Numerical simulations are so far time consuming and inaccurate due to finite-size effects in studies of steps with $Q>20$ and thus cannot give information either on fractal dimension.

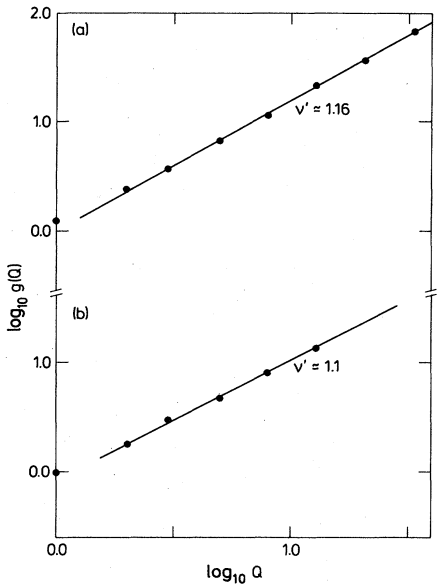

FIG. 16. Double-logarithmic plot of $g(Q)$ for Fibonacci fractions. (a) Infinite-range approximation. (b) Two-dimensional square lattice.

V. IRRATIONAL ROTATION NUMBERS AND FLUCTUATIONS

So far we have concentrated on rational rotation numbers on steps or on isolated lines in the K,Ω plane. The irrational rotation numbers can be dealt with in the infinite-range approximation, if we assume that the average phase is linear in n:

$$\langle\phi_n\rangle=n2\pi R+C\ , \tag{28}$$

i.e., all (infinitely many) C_n's are equal to a constant C. We shall consider only irrationals close to a step, either when we change Ω through $\Omega_>$ or $\Omega_<$, or when slightly below $K_c(J)$ Ω is varied through the point $\Omega_{P/Q}$ which satisifes the self-consistency for a given P/Q.

The dependence of the rotation number on the distance from these special points turns out to be equivalent to the onset of sliding motion of CDW's under strong pinning, and the linear conductivity problem of weakly pinned CDW's.[11] The connection is as follows: We write the equations of motion, Eq. (4), formally as

$$\underline{\Phi}_{n+1}=\underline{F}(\underline{\Phi}_n)\ . \tag{29}$$

If $R=P/Q$ the function $\underline{F}^{Q}(\underline{\Phi})$ has a fixed point. As Ω is changed slightly and the rotation number acquires an irrational value, the variable $\underline{\Psi}_n=\underline{\Phi}_{nQ}$ still spends most of its time close to the fixed-point value and thus moves slowly in the vicinity of it. Therefore we are allowed to replace the discrete equation for $\underline{\Psi}_n$ by its continuum version, which is equal to Eq. (3) with $m=0$ and some corrections, which are irrelevant when the rotation number is close enough to the rational P/Q.

This method of connecting the discrete and continuum dynamics close to a tangential bifurcation is a standard one.[5] If $J=0$, the discrete version locks to all rationals, whereas the continuum version has a smooth $R(\Omega)$. This difference is avoided for $J\neq 0$ and $K<1$ close enough to a step because only a finite number of steps exist. When $K>1$ and all the highest-order Q steps occur, the connection holds in the same sense as for a single circle map: the most stable points of the steps scale according to the continuum case.

We do not repeat Fisher's excellent treatment of the continuum dynamics in the infinite-range limit[11] (see also Ref. 12), but just quote the relevant results. The rotation number close to the edge is given by

$$|R-P/Q| \sim |\Omega-\Omega_{<(>)}|^{3/2} \tag{30}$$

and the steepness of the appearing step vanishes as

$$\left.\frac{dR}{d\Omega}\right|_{\Omega=\Omega_{P/Q}} \sim (K_c-K)^{1/2} . \tag{31}$$

It is remarkable that both exponents are independent of Q and on the special choice of $g(x)$.

The result (30) is subject to the following caveat: Ritala and Hertz[12] (RH) studied the fluctuations around Fisher's infinite-range approximation of the onset of sliding motion and found singular short-range corrections which affect the exponent as soon as the number of neighbors z is finite. In a Bethe approximation RH determined the exponent of Eq. (30) to be nonuniversal if $z<(1+f/J')^2$ [cf. Eq. (3)] and equal to one otherwise.

The important fluctuations in a system with only a finite number of nearest neighbors are due to nonlinearity of the dynamics and inhomogeneity of the pinning phases $\beta^{(i)}$, and they have no counterpart in ordinary phase transitions. The quantity of interest in the continuum time case is the time derivative of the intrinsic field

$$\dot{h}^{(i)}=z^{-1}\sum_{j=1}^{z}\dot{\phi}^{(i)} \tag{32}$$

which couples to the "order-parameter field" $\dot{\phi}^{(i)}$. The fluctuations in $\dot{h}^{(i)}$ behave as[12]

$$\frac{\langle(\Delta\dot{h}^{(i)})^2\rangle}{\langle\dot{h}^{(i)}\rangle^2} \sim z^{-1}|R-P/Q|^{-2/3} \tag{33}$$

and diverge for all finite z when the edge of the step is approached. Furthermore, because of the absence of such fluctuations on the step the divergence of Eq. (33) cannot be supressed by a shift in $\Omega_{<(>)}$. Note that in systems with continuous spatial variation this kind of fluctuation

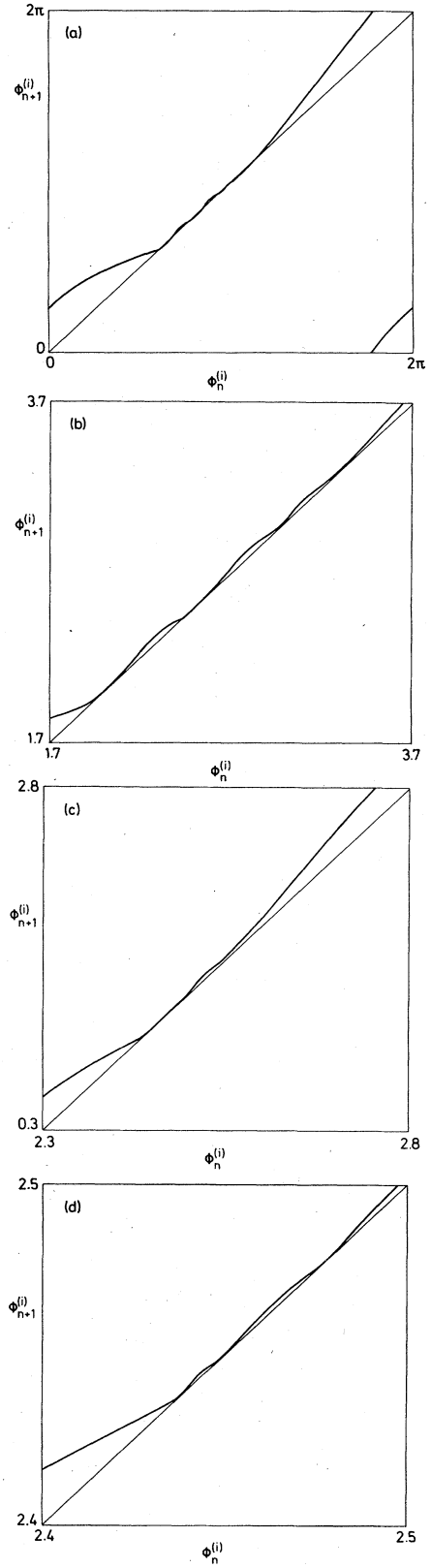

FIG. 17. Example of local return map of two-dimensional simulations. $\Omega=0.285$, $J=0.2$, and $K=0.5$. (a) Return map in interval $[0,2\pi)$. (b)—(d) Successive close-ups of (a) in regions where the change in dynamical variable is slow.

cannot exist and thus the continuum limit of the present theory is unclear. In particular, perturbation calculations of the upper critical dimension of continuum models do not say anything about the model of Eq. (3).

In this work we studied in simulations the effect of only a finite number of nearest neighbors on irrational rotation numbers. We have chosen to look at the effective local return map of a phase in the lattice. Figure 17 shows an example of such a map; the change in the internal field $h_n^{(i)}$ corresponding to the same fixed values of parameters and the same configuration of random phases $\beta^{(i)}$ is displayed in Fig. 18. We want to stress that the single-valuedness of this local return map is by no means accidental. Thus it is possible to describe also the finite-ranged system by a local equation and a self-consistent internal field. Here, however, the field is a much more complicated function of time (n) as is evident from Fig. 18. All this supports the approach by RH, but we are not able to determine accurately enough the distribution of $h_{n+1}^{(i)}-h_n^{(i)}$, the crucial quantity of RH, from our numerical data. RH predict that for the parameter values of Figs. 17 and 18 the rotation number R should depend linearly on the distance from the edge of the step. (This was used in Sec. III B; see also Figs. 10 and 12.) Numerical results, which are displayed in Fig. 19, show finite-size effects close to the transition, but seems to be in fair agreement with RH. An additional problem at the transition are the domain-wall structures,[21] which are neither taken into account in the infinite-range approximation nor in RH. To determine the role of short-range fluctuations further numerical work, including finite-size scaling, is needed.

The short-range fluctuations are important only at irrational rotation numbers. Thus the results of Secs. III and IV hold for both infinite and finite ranges of interactions as our simulations indeed show. Below K_c the short-range fluctuations are irrelevant and thus we expect the result, Eq. (31), to hold for a finite range of interactions, too. Again the numerical simulations are so noisy that the exponent cannot be determined with required accuracy.

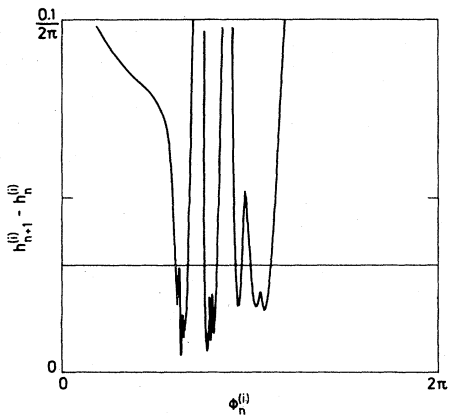

FIG. 18. Internal field, defined through Eq. (32), corresponding to return map of Fig. 17. Dashed line is infinite-range field.

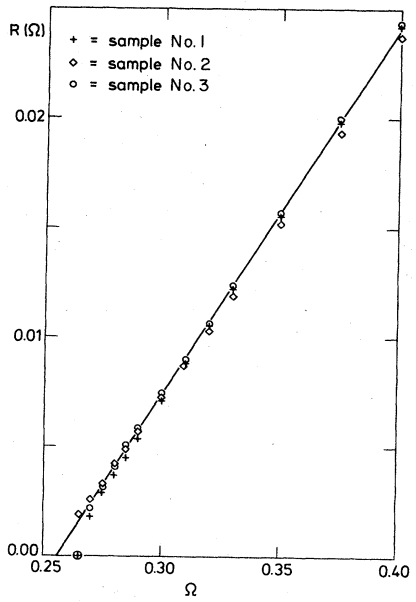

FIG. 19. $R(\Omega)$ for three different samples of size 30×30 close to the 0/1 step. $K=0.5$, $J=0.2$. Rapid jump to zero at $\Omega=0.26$ is due to finite-size effects.

VI. DISCUSSION

In this paper we have demonstrated that the dynamical properties, mode-locking structure, and bifurcations of infinitely many coupled circle maps with random phases are qualitatively different from those of a single circle map, the limit of vanishing coupling. In particular, for small values of the nonlinearity parameter we find only a finite number of exact steps, a few plateaus with small but finite slope $dR/d\Omega$, and infinitely many steps missing. Also, the complete mode-locking line changes abruptly as the coupling is turned on.

We have derived in the infinite-range approximation the novel behavior of the vanishing slope of the plateaus, Eq. (31); the critical value of the nonlinearity, Eq. (17); the width of the step near the critical nonlinearity, Eq. (20); the width of the step at the complete mode-locking line of the single circle map as the coupling is turned on, Fig. 16; and of the rotation number close to a step, Eq. (30). All these, except the last one, survive under short-range fluctuations. Numerical simulations agree quite well in most points, although the numerical accuracy is rather poor. The effect of fluctuations on irrationals is discussed in Ref. 12.

A motivation of this work has been to understand the mode-locking behavior observed in CDW materials. The recent experiments show mode locking to smallest denominator steps, "incomplete" locking of the intermediate steps (not to be confused with incomplete versus complete locking in circle maps), i.e., small but finite slope in dI/dV curves, and finally no locking at higher denominator steps.[22] This is exactly the behavior of our model with

a small value of nonlinearity parameter. Therefore we expect the other properties found in this paper to be observable in CDW experiments, too. In particular, we suggest experiments to investigate the properties, Eqs. (20) and (31). Note that our theory does not give connection between the physical quantities and the parameters of our model. However, we believe that the nonlinearity is most simply tuned by varying the amplitude of the time-dependent ac voltage.

Recently, it has been shown that mode-locking behavior similar that we have observed is found in the continuum-time—continuum-space model at finite dimension, too.[23] This suggests that our conclusions on the irrelevancy of short-range fluctuations on the step and below the critical nonlinearity are correct. However, the discrepancy between the continuous and the discrete space models on irrationals, Eq. (30) and the RH result, still remains to be settled.

There exist several open questions in our theory. The fate of the complete mode locking needs further studies. It would be interesting to determine the Feigenbaum constants[24] α and δ for the period-doubling sequence. We do not have intuitive understanding on either why the critical nonlinearity has a maximum as a function of denominator, or why $K=1$ has a special role at high values of denominators. How far can the expression Eq. (17) be pushed in J and Q?

We conclude that the dynamics studied in this paper is new and interesting and deserves more study. Many of its aspects are realized in charge-density-wave dynamics.

ACKNOWLEDGMENTS

We have benefitted from discussions with Tomas Bohr, Susan Coppersmith, John Hertz, Mogens Jensen, Mark Robbins, and Mark Sherwin.

[1]M. H. Hensen, P. Bak, and T. Bohr, Phys. Rev. Lett. **50**, 1637 (1983); Phys. Rev. A **30**, 1960 (1984).

[2]S. J. Shenker, Physica **5D**, 405 (1982).

[3]M. J. Feigenbaum L. P. Kadanoff, and S. J. Shenker, Physica **5D**, 370 (1982); D. Rand, S. Ostlund, J. Sethna, and E. Siggia, Phys. Rev. Lett. **49**, 132 (1982); Physica **8D**, 303 (1983).

[4]T. Bohr and G. Gunaratne, Phys. Lett. **113A**, 55 (1985).

[5]J. E. Hirsch, B. A. Huberman, and D. J. Scalapino, Phys. Rev. A **25**, 519 (1982); J. E. Hirsch, M. Nauenberg, and D. J. Scalapino, Phys. Lett. **87A**, 391 (1982); B. Hu and J. Rudnick, Phys. Rev. Lett. **48**, 1645 (1983).

[6]P. Bak, T. Bohr, M. H. Jensen, and P. V. Christiansen, Solid State Commun. **51**, 231 (1984).

[7]P. Alstrøm, M. H. Jensen, and M. T. Levinsen, Phys. Lett. **103A**, 171 (1984); P. Alstrøm and M. T. Levinsen, Phys. Rev. B **31**, 2753 (1985); W. J. Yeh, D. R. He, and Y. Kao, Phys. Rev. Lett. **53**, 480 (1984).

[8]V. N. Belykh, N. F. Pedersen, and O. H. Soerensen, Phys. Rev. B **16**, 4860 (1977).

[9]See, e.g., I. Iooss and D. D. Joseph, *Elementary Stability and Bifurcation Theory* (Springer, New York, 1980).

[10]G. Grüner, A. Zawadowski, and P. M. Chaikin, Phys. Rev. Lett. **46**, 511 (1981); J. W. Brill, N. P. Ong, J. C. Eckert, J. W. Savage, S. K. Khanna, and R. B. Somoano, Phys. Rev. B **23**, 1517 (1981).

[11]D. S. Fisher, Phys. Rev. Lett. **50**, 1486 (1983); Phys. Rev. B **31**, 1396 (1985); for incommensurate pinning see L. Sneddon, *ibid.* **30**, 2974 (1984).

[12]R. K. Ritala and J. A. Hertz, Phys. Scr. (to be published).

[13]G. Grüner, A. Zettl, W. G. Clark, and A. H. Thompson, Phys. Rev. B **23**, 6813 (1981).

[14]S. E. Brown, G. Mozurkewich, and G. Grüner, Phys. Rev. Lett. **52**, 2277 (1984); S. E. Brown, G. Grüner, and L. Mihaly, Solid State Commun. **57**, 165 (1986).

[15]$J=0$ case is studied in M. Ya. Azbel and P. Bak, Phys. Rev. B **30**, 3722 (1984).

[16]K. Kaneko, Prog. Theor. Phys. **69**, 1472 (1983); **72**, 480 (1984); Phys. Lett. **111A**, 1662 (1985).

[17]V. I. Arnold, Transl. Am. Math. Soc. **46**, 213 (1965).

[18]R. Thom, *Structural Stability and Morphogenesis* (Benjamin, Reading, Mass., 1975), Chap. 5.

[19]R. Perez and L. Glass, Phys. Lett. **90A**, 441 (1982); J. Belair and L. Glass, Physica **16D**, 143 (1985).

[20]P. Alstrøm, B. Christiansen, P. Hyldgaard, M. T. Levinsen, and D. R. Rasmussen, Phys. Rev. A **34**, 2220 (1986).

[21]H. Matsukawa and H. Takayama, Solid State Commun. **50**, 283 (1984); we have observed similar structures in discrete-time simulations in one- and two-dimensional models.

[22]M. S. Sherwin and A. Zettl, Phys. Rev. Lett. **32**, 5536 (1985).

[23]S. N. Coppersmith (private communication).

[24]M. J. Feigenbaum, J. Stat. Phys. **19**, 25 (1978); **21**, 669 (1979).